Reports

Evidence for Extreme Partitioning of Copper into a Magmatic Vapor Phase

JACOB B. LOWENSTERN,* GAIL A. MAHOOD, MARK L. RIVERS, STEPHEN R. SUTTON

The discovery of copper sulfides in carbon dioxide– and chlorine-bearing bubbles in phenocryst-hosted melt inclusions shows that copper resides in a vapor phase in some shallow magma chambers. Copper is several hundred times more concentrated in magmatic vapor than in coexisting pantellerite melt. The volatile behavior of copper should be considered when modeling the volcanogenic contribution of metals to the atmosphere and may be important in the formation of copper porphyry ore deposits.

THE VOLATILITY OF COPPER IN MAGMATIC systems is demonstrated by the transport of Cu in volcanic gases and the precipitation of copper sulfides, chlorides, and sulfates in fumarolic sublimates (*1, 2*). A less understood example of high-temperature transport of Cu is the association of ore-grade Cu mineralization with small, hypabyssal granitoids. Although theoretical (*3*) and experimental studies (*4, 5*) have clarified the chemical conditions necessary for the transport of Cu at high temperatures, there is little direct geological evidence for when and how Cu is extracted from magma. In this report we describe such evidence from vapor bubbles and coexisting glass within melt inclusions (*6*). We determined the Cu contents of the bubbles using an x-ray microprobe (*7*) and calculated apparent vapor/melt partition coefficients (X^{v}_{Cu}/X^{m}_{Cu}).

Melt inclusions (Fig. 1A) are small (<200 μm) blebs of melt trapped in growing phenocrysts (crystals) at high temperature and pressure in the magma chamber (*8*). The phenocrysts act as pressure vessels during eruption, preventing the inclusions from outgassing and thereby preserving samples of the preeruptive melt and its volatile components (*9*). We analyzed melt inclusions in phenocrysts from pantellerites, strongly peralkaline [$(Na_2O+K_2O)/Al_2O_3 > 1.6$] rhyolites from Pantelleria, an island volcano in the Strait of Sicily (*10*). Pantellerites are rich in Na, Fe, Cl, light rare-earth elements, Zr, Hf, U, Th, and the base metals Zn, Sn, Mo, and Pb (*11*), but they have low concentrations of Cu (5 to 10 ppm), lower than those of alkaline olivine basalt associated with the pantellerites [20 to 90 ppm (*12*)]. The low Cu contents were not caused by crystal fractionation, as Cu was not partitioned strongly into any of the phenocryst phases (*11, 13*). Volatile components can be lost, however, during eruptive degassing. By comparing trace-element concentrations in melt inclusions to those in outgassed matrix glass, we can determine if metals, as well as H_2O, CO_2, Cl, and S, were lost to the atmosphere during eruption.

We analyzed melt inclusions in quartz from samples of pantellerite lava domes at Contrade Sciuvechi, Valenza, and Gadir and from the basal section of the Green Tuff. As quartz is the last major phase to crystallize in the pantellerite magma, its inclusions are representative of melt compositions shortly before eruption. Quartz also contains extremely low contents of trace elements, and, therefore, its presence does not affect the accuracy of our inclusion analyses. We found two populations of inclusions at Pantelleria. (i) Glassy inclusions (Fig. 1B) either had visible capillaries through the quartz [hourglass inclusions (*14*)], were located in ruptured phenocrysts, or were shown by infrared (IR) spectroscopy (*15*) to be low in H_2O (0 to 1% by weight). Glassy inclusions therefore leaked and no longer retained preeruptive volatiles. (ii) Devitrified inclusions were opaque, cryptocrystalline mixtures of sanidine, cristobalite, and alkali amphibole (Fig. 1C). We remelted the

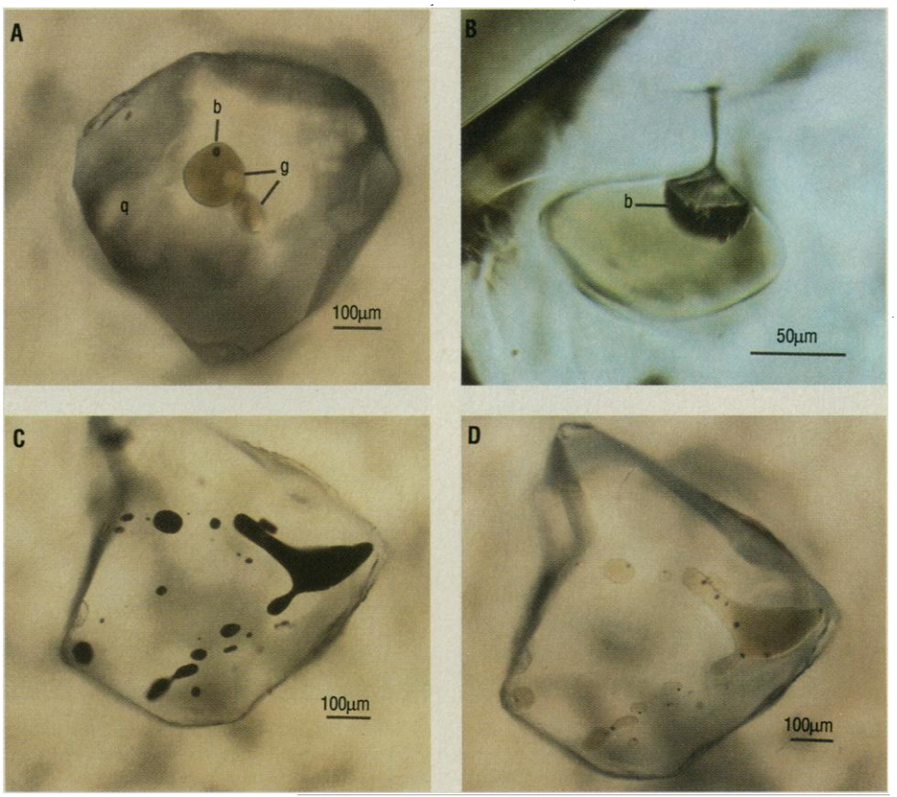

Fig. 1. Optical photographs of melt inclusions. (**A**) Two remelted inclusions showing glass (g) trapped in quartz (q) and an associated vapor bubble (b). (**B**) In a leaked glassy inclusion, a capillary connects the low-H_2O glass and a vapor bubble to the outside of the host quartz. (**C**) Devitrified inclusions in quartz can be heated and cooled to produce remelted inclusions (**D**) that are hydrous and contain several small vapor bubbles.

J. B. Lowenstern and G. A. Mahood, Department of Geology, Stanford University, Stanford, CA 94305.
M. L. Rivers and S. R. Sutton, Department of Applied Science, Brookhaven National Laboratory, Upton, NY 11973.

*To whom correspondence should be addressed.

inclusions by heating the host phenocrysts to 825°C at 1-atm external pressure (*16*). By reheating the inclusions in closed-system pressure vessels (the quartz hosts), we recreated liquidus conditions. By then rapidly cooling the samples to glass, we prevented the devitrification of inclusions that had occurred in nature. The remelted inclusions (Fig. 1D) contained glasses of major element compositions identical to those of the matrices. They had high H_2O contents that varied little within samples from individual eruptive units (for example, 1.82%, $n = 13$ inclusions, $\sigma = 0.12\%$ for a sample from Contrada Sciuvechi); these data indicate that the devitrified inclusions retained preeruptive volatiles (*15*).

Remelted inclusions contained one or more vapor bubbles (<1 to 20 μm; Fig. 1, A and D). Had the quartz hosts trapped a single homogeneous melt phase, these would be shrinkage bubbles formed during cooling of the melt (*8*), and their size would scale to the volumes of the inclusions. Alternatively, some abnormally large bubbles could represent original entrapment of a two-phase system: melt plus vapor. Such a magmatic vapor (*17*) would have been in equilibrium with the melt at magmatic conditions [~825°C and ~100 MPa (*18*)]. Because the inclusions cooled and devitrified after eruption and were remelted in the laboratory, the origin of any individual vapor bubble is not obvious. During remelting, magmatic bubbles may have been partially resorbed and then reappeared as many smaller bubbles on cooling; some may have shrunk during cooling. Bulk analyses of melt inclusions can reveal which have trapped magmatic vapor.

Devitrified and remelted inclusions, as well as glassy inclusions and matrix, were analyzed with the x-ray microprobe installed on beamline X26A at the National Synchrotron Light Source at Brookhaven National Laboratory in Upton, New York. This instrument is used for nondestructive, quantitative analysis of small (10 μm) samples. Because the photon beam penetrates deeply compared with electron, proton, or ion beams, it permits analysis of small features such as fluid and mineral inclusions beneath the surface of a sample (*7, 19*).

X-ray microprobe analyses showed that both outgassed matrix glass and leaked, glassy inclusions (Fig. 1B) contained 3 ± 1 ppm of Cu. X-ray spectra were also collected for 20 devitrified inclusions located entirely within doubly polished quartz phenocrysts from a pantellerite lava (Contrada Sciuvechi). Because the size of the photon beam was smaller than the inclusions, the movable stage was programmed to raster the entire inclusion through the beam, thereby collecting a single spectrum approximating the integrated trace-element content of the inclusion. These bulk analyses showed that, of the 20 inclusions, 18 contained 20 ± 10 ppm of Cu; they were termed Cu-poor. Two contained significantly more Cu, 100 ± 20 and 170 ± 20 ppm, but, because these Cu-rich, devitrified inclusions were opaque, it was not possible to determine optically where the anomalous Cu resided.

To identify the location of the Cu, we performed analyses on transparent, remelted inclusions prepared as doubly polished wafers. Bulk analyses also showed Cu-poor and Cu-rich inclusions, with some inclusions containing up to 300 ppm of Cu. We produced inclusion maps (Fig. 2) by moving the stage in 10-μm steps and counting x-rays from each pixel for 20 s. These maps showed that all analyzed elements except Cu were homogeneous within the inclusions. Although the Cu content was uniformly low throughout Cu-poor inclusions, it was extremely heterogeneous within Cu-rich inclusions and appeared to reside within vapor bubbles and at the boundary between glass and quartz host. The Cu content of the glass within all remelted inclusions was 20 to 30 ppm, regardless of whether the inclusion was Cu-rich or Cu-poor. This also indicates that most of the Cu in Cu-rich remelted inclusions resided in vapor bubbles. Cu-rich bubbles and inclusions were found in all four of the pantellerite units, as well as in a trachyte lava.

In order to determine the chemical components in the vapor bubbles, we carried out a microanalytical study of a remelted inclusion-bubble pair (Fig. 3A) in quartz from a lava flow at Contrada Valenza. The bubble was 22 μm in diameter, much larger than most bubbles in inclusions of comparable size (compare to Fig. 1A); the large size of the bubble supports the idea that two phases

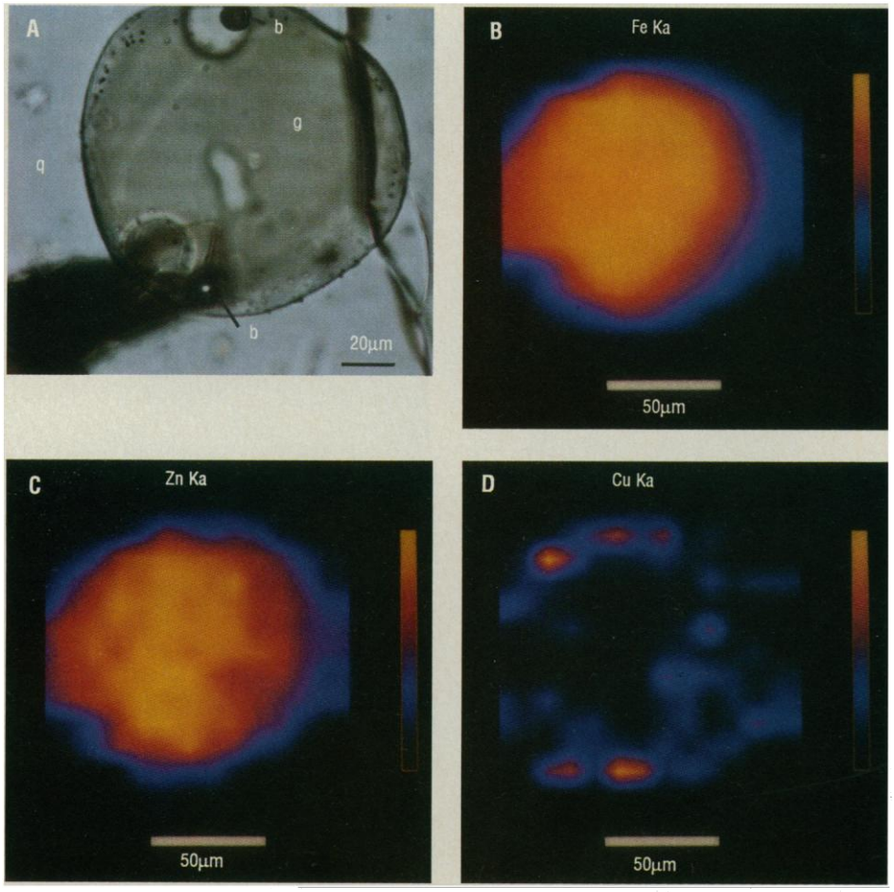

Fig. 2. Optical and x-ray maps of a doubly polished, remelted 55-μm-thick inclusion (g) in quartz (q). (**A**) Abundant small, dark, vapor bubbles are located at the inclusion periphery, as are two larger vapor bubbles (b). The black feature at the lower left, extending from the lower bubble, is carbon paint. Three light-colored features at top, center, and lower left are residual quartz growths (r) that do not completely dissolve during the remelting process. X-ray microprobe maps of this inclusion are color-contoured for Fe (**B**), Zn (**C**), and Cu (**D**), respectively. Yellow represents the highest count rate and black the lowest (as shown in color bars). Fe and Zn are homogeneous in the inclusion. Cu is absent in the quartz and heterogeneous within the inclusion and is located at the inclusion periphery, apparently in vapor bubbles.

were originally trapped in the inclusion and that this bubble did not form solely by shrinkage. The bubble was opened by Ar ion milling; subsequent imaging with a scanning electron microscope (SEM) showed mineralization on the bubble wall that was clearly vapor phase in origin (Fig. 3, B to D). The minerals were chlorides (of Na?) and copper sulfides that apparently precipitated from a vapor when the sample cooled in the laboratory.

IR spectroscopy indicated that the main constituent of these bubbles may be CO_2. The large Cu-rich bubbles from remelted pantellerite inclusions showed doublets at 2350 cm^{-1}, corresponding to CO_2 vapor (*20*). Although CO_2 was a significant component within the vapor, its concentration could not be quantified because the IR path length was poorly constrained in such small bubbles. The bubbles therefore contained at least CO_2, Cl, Na(?), Cu, and S, although necessarily as different species than were present at high temperature. In addition, H_2O was likely present in the gas, but the lack of a liquid phase in the bubble and negligible H_2O vapor peaks in the IR spectra indicated that it was subordinate to CO_2. Additional evidence that H_2O did not partition strongly into any vapor or crystalline phase was the linear, positive correlation between concentrations of H_2O in remelted inclusions and whole rock incompatible metal concentrations (*15*).

We consider three scenarios for the formation of the melt inclusions and their Cu-rich bubbles:

1) Cu was homogeneously dissolved in melt trapped in quartz, and the Cu later partitioned into shrinkage bubbles. This theory is inconsistent with the observation that bulk analyses of some devitrified and remelted inclusions indicated very high Cu contents.

2) Cu was inhomogeneously dissolved in the melt, resulting in entrapment of the observed Cu-poor and Cu-rich melt inclusions. Cu then partitioned mostly into shrinkage bubbles. This requires a mechanism for fractionating Cu (and only Cu, as other metals are homogeneous) in the magma chamber, on a hand-sample scale, without vapor transport.

3) Cu resided mostly within a vapor phase in equilibrium with pantellerite melt in the magma chamber. Vapor bubbles were trapped randomly along with melt during formation of some inclusions (*17*). This last hypothesis most easily accounts for the following results: (i) the low Cu content of pantellerite matrix glass and leaked, glassy inclusions (3 ± 1 ppm), which appear to have lost Cu during open-system degassing; (ii) the slightly higher Cu contents (20 ± 10 ppm) of most devitrified and remelted inclusions, which did not undergo eruptive degassing; and (iii) the observation that most bubbles in Cu-rich, remelted inclusions were larger than the vapor (shrinkage) bubbles in Cu-poor, remelted inclusions.

We performed x-ray microprobe analyses on individual vapor bubbles in remelted inclusions to determine apparent vapor/melt partition coefficients (PCs) for Cu. We determined the mass of Cu in a bubble by orienting the photon beam to intersect and fluoresce the bubble contents. Calibration was relative to two semi-independent techniques (*7, 19*), an internal standard (Fe in the glass: PC I in Table 1) and an external standard (PC II). We converted the mass of Cu to concentration in the vapor by determining the bubble volume and by assuming a vapor density of 0.4 ± 0.1 g/cm^3 (*21*) and a Cu content in the glass of remelted inclusions of 20 ppm.

Table 1 lists calculated PCs for Cu-rich bubbles that apparently contained a high ratio of magmatic vapor to shrinkage bubble. Values for PC I ranged from 400 to 1600 compared to 200 to 700 for PC II. The twofold difference between the techniques is similar to our reported uncertainties and is consistent with analysis accuracy within a factor of 2 (*22*). The values are generally consistent with the amount of Cu

Table 1. Apparent vapor/melt partition coefficients (PC) for Cu calculated from analyses of coexisting vapor bubbles and remelted inclusion glass; n.a., not analyzed.

Sample number	Bubble diameter (μm)	Bubble depth (μm)	PC I	PC II
Sciu 2	10.5 ± 1	8 ± 2	700 ± 500	200 ± 100
Sciu 4	8.5 ± 1	1 ± 0.5	1100 ± 800	500 ± 300
Sciu 24a	8.5 ± 1	10 ± 2.5	400 ± 300	200 ± 100
Sciu 24b	10 ± 1	8 ± 2	700 ± 500	200 ± 100
Val 15a	9 ± 1	3 ± 0.8	800 ± 600	400 ± 200
Val 15b	10 ± 1	10 ± 2.5	1600 ± 1100	700 ± 400
Gad 1*	15 ± 1	5 ± 1	600 ± 300	n.a.

*Inclusion in sanidine.

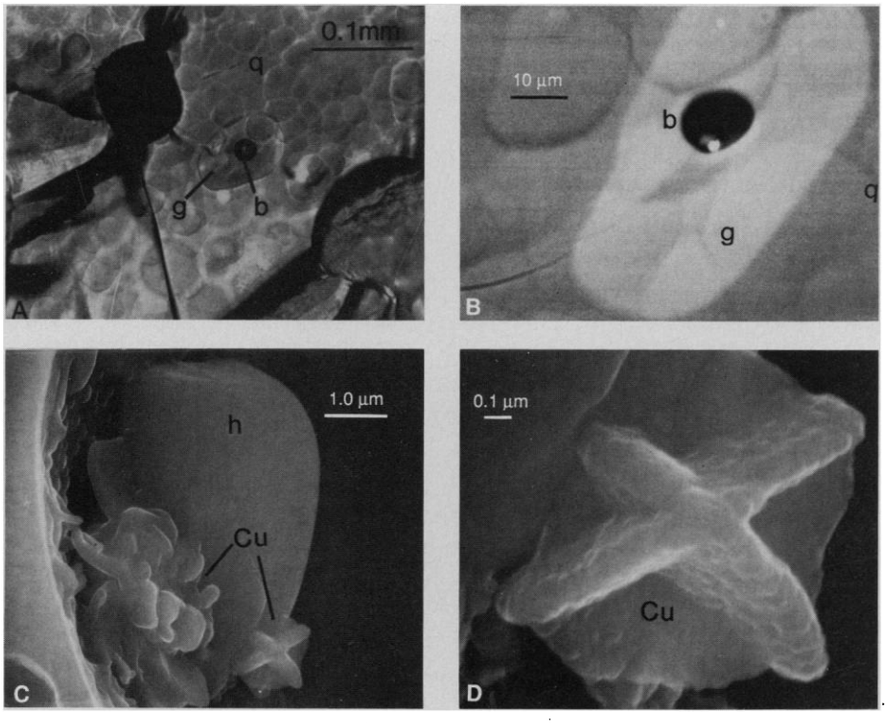

Fig. 3. Optical photograph (**A**) of a large, unexposed vapor bubble (b) in a remelted inclusion (g) trapped in quartz (q). The mottled texture was created during the Ar ion milling process used to expose the bubble for viewing under the SEM. A backscattered electron image of the same inclusion (**B**), tilted 45°, shows the quartz, glass, and bubble (exposed). Inside the bubble is high atomic number, vapor-phase mineralization (bright spot) shown by secondary electron imaging (**C** and **D**). The chloride (h) of a light element, probably Na, and a platy copper sulfide (Cu) were identified by energy-dispersive analysis.

visible in the opened bubble shown in Fig. 3. For example, estimating 3 μm^3 of CuS in that bubble and calculating the mass of vapor that would be present in a bubble of that volume (*21*), we obtained a PC of about 200. Given that much of the Cu may have been lost during ion milling, this value would be a minimum. The remelting process may have affected our results somewhat but is unlikely to alter the PCs by more than our reported uncertainties.

The experiments showed that Cu was strongly partitioned into vapor bubbles, such that apparent PCs may reach well over 1000. These values are higher than those determined by Candela and Holland (*4*) for the partitioning of Cu between high-silica rhyolite and Cl-rich aqueous fluid. In that study, at 750°C and 140 MPa, the PC varied linearly with Cl concentration in the vapor and reached 50 for a 4.6 molal (~16% by weight) Cl solution. Our higher values could be due to differences in melt composition, and to the higher temperature and lower pressure in this study, conditions that may favor volatilization. It is also possible that the apparent high CO_2/H_2O ratio of the vapor in these peralkaline rhyolites would minimize the amount of Cl bound up in gaseous HCl; therefore, Cl would be freed for the transport of Cu.

Unlike Cu, Zn content in the melt increases with differentiation, consistent with its stability in the crystallizing melt and its apparent absence in the magmatic vapor (Figs. 2C and 3). The contrasting behavior of Cu and Zn may be due to their different valences and ionic radii, as the small, univalent Cu ion may not fit easily into melt structural sites, favoring its volatility (*4*). Lepel *et al.* (*1*) studied aerosols produced during the 1976 dacite eruption of Augustine volcano and found that the Cu/Zn ratio in the aerosols fell with time by a factor of 16, consistent with the stronger partitioning of Cu than Zn into magmatic vapor.

Extreme volatility of Cu has been reported from eruptions of widely differing composition, notably during eruptions in which abundant juvenile material was degassed (*23*). Because Cu can be greatly concentrated in magmatic vapor, voluminous eruptions may significantly impact the long-term, trace-metal budget of the atmosphere. The annual volcanogenic contribution of Cu to the atmosphere has been estimated as only 27% of anthropogenic additions, which arise mostly from metallurgical processing (*24*). These figures, however, are based on enrichment factors applicable to quiet degassing and low-output eruptions (*1, 25*). This study shows that a single major eruption can add 50 times more Cu to the atmosphere than the annual global output of quietly degassing volcanoes. We calculate that the eruption of the Green Tuff 45,000 years ago at Pantelleria released 5×10^5 tons of Cu during catastrophic degassing (*26*), roughly ten times the annual anthropogenic contribution of Cu to the atmosphere. Although the lifetime of Cu species in the atmosphere is short (*27*), and large volcanic eruptions are infrequent, the mass of metals released during these eruptions will be significant in the long-term global cycling of metals.

In plutonic environments, vapors evolved from magma may be available for ore deposition. Candela (*28*) stated that because Cu appears to act compatibly as a result of partitioning into magmatic sulfides, it will be removed from a melt most efficiently if vapor saturation occurs before significant crystallization. Such conditions could be met by a shallow magma body with high H_2O content or by the presence of low-solubility gases such as CO_2. Our discovery of Cu- and CO_2-bearing vapor in pantellerites with only 10% crystals and in rhyolites with 2% phenocrysts [at the Valley of Ten Thousand Smokes (*29*)] demonstrates that early vapor saturation can occur. It also suggests that crystallization-induced volatile saturation [second boiling (*30*)] may not be necessary for the production of Cu-rich fluids.

The low solubility of CO_2 in silicate melts at low pressure means that magmas may commonly be saturated with respect to a vapor phase (*31*). Although CO_2 would not actively complex Cu, its presence as bubbles would provide a low-density volatile phase into which Cu could partition, most likely as CuCl (*3, 4, 32*). This volatile phase would then evolve during crystallization, cooling, and influx of meteoric H_2O to form the acidic brines associated with ore deposition (*33*).

REFERENCES AND NOTES

1. E. A. Lepel, K. M. Stefansson, W. H. Zoller, *J. Geophys. Res.* **83**, 6213 (1978).
2. R. E. Stoiber and W. I. Rose, *Geochim. Cosmochim. Acta* **38**, 495 (1974).
3. K. B. Krauskopf, *Econ. Geol.* **59**, 22 (1964).
4. P. A. Candela and H. D. Holland, *Geochim. Cosmochim. Acta* **48**, 373 (1984).
5. R. D. Ryabchikov, G. P. Orlova, A. S. Efimov, G. E. Kalenchuk, *Geokhimiya* **9**, 1320 (1980).
6. We use the term "vapor" for a high-temperature (800°C), low-density (~0.4 g/cm³) volatile magmatic phase with limited capacity as a solvent. "Melt" refers to the liquid silicate phase, which, together with crystals and vapor, composes magma.
7. F. Q. Lu, J. V. Smith, S. R. Sutton, M. L. Rivers, A. M. Davis, *Chem. Geol.* **75**, 123 (1989).
8. E. Roedder, in *Fluid Inclusions*, vol. 12 of *Reviews in Mineralogy*, P. H. Ribbe, Ed. (Mineralogical Society of America, Washington, DC, 1984), pp. 473–501.
9. A. T. Anderson *et al.*, *Geology* **17**, 221 (1989); S. Takenouchi and H. Imai, *Econ. Geol.* **70**, 750 (1975).
10. G. A. Mahood and W. Hildreth, *Bull. Volcanol.* **48**, 143 (1986).
11. Analysis of Sciuvechi lava: SiO_2 = 69.3% (by weight); Al_2O_3 = 8.18%; Fe_2O_3 = 8.6%; MgO = 0.1%; CaO = 0.34%; Na_2O = 6.76%; K_2O = 4.45%; Cl = 0.77%; La = 263 ppm; U = 13.3 ppm; Zr = 2050 ppm [data from G. A. Mahood and J. A. Stimac, *Geochim. Cosmochim. Acta* **54**, 2257 (1990)]. All iron was analyzed as Fe_2O_3.
12. G. A. Mahood, unpublished emission spectroscopic analyses; L. Villari, *Bull. Volcanol.* **38**, 680 (1974).
13. J. B. Lowenstern, unpublished x-ray microprobe analyses of phenocrysts.
14. A. T. Anderson, *IUGG XIX General Assembly Abstracts* (International Union of Geodesy and Geophysics, Vancouver, 1987), p. 400.
15. J. B. Lowenstern and G. A. Mahood, in *V. M. Goldschmidt Conference Program and Abstracts* (Geochemical Society, Washington, DC, 1990), p. 62.
16. Devitrified inclusions in their quartz hosts were placed in a Pt crucible and heated with a DelTech furnace at 400°C per hour to 825°C; then they were held at that temperature for 4 to 6 hours. The short duration of the experiments ensured that H_2 loss by diffusion through the quartz hosts was trivial. There was no noticeable dissolution of the hosts by included melt. In order to avoid cracking of the host phenocrysts, we cooled the system at 50°C per hour until the crucible was extracted from the oven at 625°C.
17. E. Roedder, *Am. Mineral.* **50**, 1746 (1965).
18. G. A. Mahood, *J. Geophys. Res.* **89**, 8540 (1984); G. Benhamou and R. Clocchiatti, *Bull. Soc. Fr. Mineral. Crystallogr.* **99**, 111 (1976).
19. The synchrotron source provided an intense x-ray beam that was collimated to an 8 by 8 μm spot and used to excite x-ray fluorescence in the sample. The incident beam had a continuous energy spectrum with usable flux between 4 and 30 keV. Spectra were gathered by a Si(Li) detector located at 90° to the incident beam. Trace-element concentrations were calculated by normalization to the Fe Kα x-ray, as Fe is homogeneously distributed throughout the inclusion and its concentration can be independently determined by electron microprobe analysis. We also calibrated with an external standard, SRM 3171 on a Millipore filter, described in B. M. Gordon *et al.*, *Nucl. Instrum. Methods* **45**, 527 (1990).
20. R. Aines, J. B. Lowenstern, G. A. Mahood, *Eos* **71**, 1699 (1990).
21. For the vapor density value it is assumed that there is ideal behavior of the presumed constituents (CO_2, HCl, H_2S, SO_2, NaOH, CuCl, and H_2O) at 100 MPa and 800°C, in ratios consistent with the relative volumes of condensed phases in Fig. 3D. The calculated density is fairly insensitive to the ratios of the constituent species (except CuCl, which is minor) because of their similar molecular weights.
22. We calculated uncertainties in PCs by propagating the errors associated with sample thickness, bubble volume and depth, vapor density, beam diameter, and x-ray analyses through the calculations. Experimental details and calculations are available upon request from J.B.L.
23. K. J. Murata, *Am. J. Sci.* **258**, 769 (1960); A. H. Delsemme, *Acad. R. Sci. Outre-Mer (Brussels) Bull. Seances D* **6**, 507 (1960).
24. J. O. Nriagu, *Nature* **338**, 47 (1989).
25. P. Buat-Menard and M. Arnold, *Geophys. Res. Lett.* **5**, 245 (1978).
26. Assumes outgassing of 7 km^3 of magma and Cu concentrations of 35 ppm in preeruptive melt and vapor and 3 ppm in the matrix glass, based on x-ray microprobe analyses. Lower partition coefficients than those determined in this study (30) will still result in similar losses, given open-system degassing.
27. J. O. Nriagu, in *Copper in the Environment*, J. O. Nriagu, Ed. (Wiley, New York, 1979), pp. 43–76.
28. P. A. Candela, in *Ore Deposits Associated with Magmas*, vol. 14 of *Reviews in Economic Geology*, J. A. Whitney and A. J. Naldrett, Eds. (Society of Economic Geologists, El Paso, TX, 1989), pp. 223–233.
29. J. B. Lowenstern, *Eos* **71**, 1690 (1990).
30. C. W. Burnham, in *Geochemistry of Hydrothermal Ore Deposits*, H. L. Barnes, Ed. (Wiley, New York, 1979), pp. 71–136.

31. J. Holloway, *Geol. Soc. Am. Bull.* **87**, 1513 (1976).
32. R. B. Symonds, W. I. Rose, M. H. Reed, F. E. Lichte, D. L. Finnegan, *Geochim. Cosmochim. Acta* **51**, 2083 (1987).
33. R. W. Henley and A. McNabb, *Econ. Geol.* **73**, 1 (1978).
34. We thank R. Aines and S. Newman for help with IR spectroscopy and P. Candela, M. Einaudi, K. Krauskopf, J. Peck, and J. Stebbins for reviews. This research was funded through National Science Foundation grant EAR 8805074 to G.A.M., grant EAR 8915699 to M.L.R., National Aeronautics and Space Administration grant NAG 9-106 to S.R.S., the McGee Fund of the Stanford School of Earth Science, and the Department of Energy, Division of University and Industry Programs, Office of Energy Research.

9 January 1991; accepted 15 April 1991

Did the Breakout of Laurentia Turn Gondwanaland Inside-Out?

PAUL F. HOFFMAN

Comparative geology suggests that the continents adjacent to northern, western, southern, and eastern Laurentia in the Late Proterozoic were Siberia, Australia-Antarctica, southern Africa, and Amazonia-Baltica, respectively. Late Proterozoic fragmentation of the supercontinent centered on Laurentia would then have been followed by rapid fan-like collapse of the (present) southern continents and eventual consolidation of East and West Gondwanaland. In this scenario, a pole of rotation near the Weddell Sea would explain the observed dominance of wrench tectonics in (present) east-west trending Pan-African mobile belts and subduction-accretion tectonics in north-south trending belts. In the process of fragmentation, rifts originating in the interior of the Late Proterozoic supercontinent became the external margins of Paleozoic Gondwanaland; exterior margins of the Late Proterozoic supercontinent became landlocked within the interior of Gondwanaland.

THE INTERVAL ENCOMPASSING THE Vendian to Cambrian transition [0.7 to 0.5 billion years ago (Ga)] is perhaps the most enduring enigma in historical geology. The advent and subsequent evolutionary explosion of metazoa were accompanied by extreme fluctuations in sea level, global climate, and the isotopic and chemical compositions of seawater (*1–3*). That these changes are related to the fragmentation of a Late Proterozoic supercontinent (*4*) is an idea that stemmed from the observation that rifting and continental breakup occurred contemporaneously around the margins of Laurentia (North America and Greenland), Baltica (Baltic shield and Russian platform), Siberia, and parts of Gondwanaland (*5–7*). However, the relation of the hypothetical supercontinent to the continents forming Gondwanaland (South America, Africa, Arabia, India, Antarctica, and Australia) is unresolved because reliable paleomagnetic data for the interval are sparse. In most reconstructions of the Late Proterozoic supercontinent, Gondwanaland is treated as a coherent entity (*1, 6, 8–11*), despite evidence that its consolidation was broadly contemporaneous with fragmentation of the northern continents (*12, 13*). Not surprisingly, some question the reality of a supercontinent that may have disintegrated before it had formed. In the absence of sea-floor magnetic anomalies, pre-Mesozoic continental reconstructions are necessarily speculative. However, correlation of Precambrian orogenic belts that were once continuous but are now truncated at modern or ancient continental margins provides a means of establishing former linkages between separated continents. On the basis of such evidence, I present a qualitative but testable model for the breakup of a Late Proterozoic supercontinent centered on Laurentia and the subsequent assembly of Paleozoic Gondwanaland.

Northeastern Siberia (all directions refer to present-day coordinates) has been proposed as the conjugate margin to southwestern Laurentia in the Late Proterozoic on geological (*14*) and paleomagnetic (*15*) grounds. The evidence is permissive but not conclusive. U-Pb zircon geochronology indicates that the Anabar and western Aldan shields (Fig. 1A) of Siberia consist of crust that formed before 3.0 Ga and underwent high-grade metamorphism and anatexis at 2.8 to 2.6 Ga and again at 2.0 to 1.9 Ga (*16*). In Laurentia, only the Thelon-Taltson magmatic zone (Fig. 1A) in northwest Canada has such a history (*17*), but this zone is truncated beneath the plains of east-central Alberta and does not appear to reach the Cordillera (*18*). However, the zone does extend northward where it is truncated by the Paleozoic Franklin orogen in the Arctic (*17*). Thus, if the Anabar and Thelon-Taltson belts were originally connected, Siberia was most likely conjugate to the Arctic (*19*) margin of Laurentia (Fig. 1A).

Jefferson (*20*) proposed that western Laurentia was flanked in the Late Proterozoic by the eastern margin of the Australian craton together with the margin of the East Antarctic craton corresponding to the Transantarctic Mountains (Fig. 1A). This proposal stemmed from comparative Late Proterozoic stratigraphy of the respective Australian and Laurentian margins (*20*). Recently, Moores (*21*) and Dalziel (*22*) have bolstered the restoration and fixed its position by pointing out that a tectonic boundary equivalent to the Grenville orogenic front of west Texas reappears in Antarctica near the east coast of the Weddell Sea (Fig. 1A). Moores (*21*) suggested that the Grenvillian (1.3 to 1.0 Ga) belt loops back around the East Antarctic craton (by way of the Eastern Ghats of India) into the Albany-Fraser belt (Fig. 1A) of southwest Australia (*23*). The reconstruction implies that the northwest corner of Laurentia lay adjacent to north-central Australia in the Late Proterozoic. There are indeed remarkable parallels in Early Proterozoic geology and U-Pb geochronology between the Wopmay orogen in northwest Canada and the Mount Isa, Pine Creek, Tennant Creek, and Halls Creek inliers of northern Australia (Fig. 1A). The main orogenic event in each area occurred from 1.90 to 1.88 Ga—the Calderian orogeny in Canada (*24*) and the Barramundi orogeny in Australia (*25*). Each area experienced intense, mainly felsic volcanism and plutonism from 1.88 to 1.84 Ga (*26, 27*), and the felsic magmas were derived from crustal sources having Nd model ages of 2.4 to 2.0 Ga (*28, 29*). The comparison not only supports the proposed reconstruction (*20–22*) but also implies that northwest Laurentia, east Antarctica, and the Australian craton were fellow travelers from 1.9 until 0.6 Ga (*30*).

If East Gondwanaland (India-Australia-Antarctica) separated from western Laurentia, then which continent or continents lay adjacent to eastern and southern Laurentia before the opening of the Iapetus Ocean? Earlier works have advocated northwest Africa (*8*), western South America (*6*), Arabia (*7, 15*), and Baltica (*31*). Pre-Grenvillian tectonic zones provide piercing points that pin Baltica adjacent to northwest Britain (*31*), which was then a part of Laurentia off southeast Greenland (Fig. 1A). To the south, the Appalachian and Ouachita margins of Laurentia are confined to the Grenville orogen. Therefore, cratons that are bordered by Grenvillian belts are more likely to have been conjugate to southeastern and

Continental Geoscience Division, Geological Survey of Canada, Ottawa, Ontario, K1A 0E8.